oxidations, resulting in tin-metal bond cleavage. The oxidation products for the triphenyltin adducts are the solvent adducts of the transition-metal cation and the triphenyltin cation. When M = $Mn(CO)_5$, this oxidation is chemically reversible. Oxidation of the diphenyltin-bridged compounds results in cleavage of only one metal-tin bond, to give the metal cation and a base-stabilized stannylene cation. Analogous chemistry was observed for the related compounds $[Mn(CO)_5]_3SnPh$ and $[Mn(CO)_5]SnPh_2[CpFe(CO)_2]$. Experimental observations suggest that the latter compound is oxidized via an ECE mechanism.

Compounds in this series also undergo net one- or two-electron reductions and concomitant rupture of the tin-metal bonds. The triphenyltin adducts yield the monomeric metal anions and, in the diiron case, the triphenylstannate anion upon reduction. Reduction of the triphenyltin adduct of $CpMo(CO)_3$ yields Sn_2Ph_6 as the final tin product. The diphenyltin-bridged compounds are reduced to the transition-metal anions and an unreduced tin product, possibly $[SnPh_2]_n$. Infrared spectral data imply that reductions of the latter compounds proceed via terminal diphenyltin stannate anion adducts of the transition-metal moieties, e.g., $CpFe(CO)_2SnPh_2^-$.

The studies presented in this work demonstrate the utility of infrared spectroelectrochemistry toward the interpretation of non-Nernstian electrode processes. The unambiguous identification of electrogenerated species, as well as the ability to monitor their subsequent chemistry, is greatly facilitated via this technique.

Acknowledgment. J.P.B. thanks the University of Minnesota Graduate School for a Stanwood Johnson Memorial Fellowship and the University of Minnesota Chemistry Department for a departmental fellowship sponsored by 3M. The FT-IR spectrometer was purchased with funds provided by the NSF (Grant No. CHE 8509325). This work was funded in part by an additional grant from 3M.

Registry No. TBAH, 3109-63-5; $[CpMo(CO)_3]_2$, 60974-85-8; $[CpMo(CO)_3]SnPh_3$, 12100-85-5; $[CpMo(CO)_3]_2SnPh_2$, 12101-39-2; $[Mn(CO)_5]_2$, 10170-69-1; $[Mn(CO)_5]SnPh_3$, 14405-84-6; $[Mn(CO)_5]_2SnPh_2$, 15219-82-2; $[Mn(CO)_5]_3SnPh$, 15219-80-4; $[CpFe(CO)_2]_2$, 12154-95-9; $[CpFe(CO)_2]SnPh_3$, 12132-09-1; $[CpFe(CO)_2]_2SnPh_2$, 12100-78-6; $[Mn(CO)_5]SnPh_2[CpFe(CO)_2]$, 42867-99-2; $CpMo(CO)_3$, 12079-69-7; $Mn(CO)_5$, 15651-51-1; $CpFe(CO)_2$, 55009-40-0; $CpMo(CO)_3SnPh_2(CH_3CN)_2^+$, 129447-88-7; $Mn(CO)_5SnPh_2(CH_3CN)_2^+$, 129447-89-8; $CpFe(CO)_2SnPh_2(CH_3CN)_2^+$, 129447-90-1; $[CpMo(CO)_3]^-$, 12126-18-0; $[Mn(CO)_5]^-$, 14971-26-7; $[CpFe(CO)_2]^-$, 12107-09-4; CH_3CN, 75-05-8.

Supplementary Material Available: A table of double-step chronocoulometry data and diffusion coefficients, figures showing cyclic voltammograms of $[Mn(CO)_5]_2SnPh_2$, $[Mn(CO)_5]SnPh_2[CpFe(CO)_2]$, and $[CpFe(CO)_2]SnPh_2$, and plots of IR spectroelectrochemical data for $[Mn(CO)_5]_3SnPh$, $[CpMo(CO)_3]_2SnPh_2$, and $CpFe(CO)_2SnPh_3$ (7 pages). Ordering information is given on any current masthead page.

Contribution from the Institut für Anorganische Chemie,
Universität Essen, D-4300 Essen, Federal Republic of Germany

Synthesis, Properties, and Structural Investigations of 1,3,2-Diazaborolidines and 2,3-Dihydro-1*H*-1,3,2-diazaboroles

Günter Schmid,* Michael Polk, and Roland Boese

Received February 14, 1990

A series of variously substituted 1,3,2-diazaborolidines have been prepared by different methods. 1,3-Diisopropyl-2-methyl-1,3,2-diazaborolidine (**1a**), 1,3-diethyl-2-methyl-1,3,2-diazaborolidine (**2a**), 1-ethyl-2,3-dimethyl-1,3,2-diazaborolidine (**3a**), and 1,2,3-trimethyl-1,3,2-diazaborolidine (**4a**) are formed from the corresponding lithiated ethylenediamines and CH_3BBr_2 in diethyl ether (method C). 2-Methyl-1-(trimethylsilyl)-1,3,2-diazaborolidine (**5a**), 1-*tert*-butyl-2-methyl-1,3,2-diazaborolidine (**6a**), and 1-isopropyl-2-methyl-1,3,2-diazaborolidine (**7a**) can be prepared either by method C, by method A, using the ethylenediamines and $H_3CB[N(CH_3)_2]_2$ to eliminate $HN(CH_3)_2$, or by method B, starting with CH_3BBr_2, NR_3, and the corresponding ethylenediamines. The unsaturated 2,3-dihydro-1*H*-1,3,2-diazaboroles **1b**–**7b** are synthesized by catalytic dehydrogenation in either liquid (**1b**–**3b**) or gaseous (**4b**–**7b**) state. Diazaboroles can act as 6-π-electron donors in $Cr(CO)_3$ complexes. **1b**–**4b** react with $(CH_3CN)_3Cr(CO)_3$ under various conditions to form the corresponding complexes **1c**–**4c**. The monosubstituted rings **5b**–**7b** are not suited to form stable $Cr(CO)_3$ complexes. One of the two rings in **8** can be combined with a $Cr(CO)_3$ fragment to give **9**. The yellow 1*H*-1,3,2-diazaborole–tricarbonylchromium complexes **1c**–**4c** decompose slowly at room temperature. 2,3-Dihydro-2-methyl-1,3-bis(trimethylsilyl)-1*H*-1,3,2-diazaborole (**10**) can be metalated at one N atom by $NaNH_2$ and K(O-*t*-Bu) to give the salts **11a** and **11b**. These alkali-metal derivatives can easily be protonated by HCl or CH_3OH to form the N–H derivative **5b**. X-ray structure analyses have been performed on the diazaborolidines **2a** and **4a** and on the diazaboroles **1b**, **2b**, **4b**, and **8**. The structures of **2a** and **4b** have been determined at two different temperatures. **1b**, **2b**, and **2a** crystallize in the monoclinic space groups $P2_1/n$, $P2_1/c$, and *Cc*, respectively. **4a** crystallizes hexagonally in the space group $P3_2$; **4b**, tetragonally in the space group $P4_3$. X–X-Difference electron densities of **4a**, **2a**, and **4b** show that the B–N bonds in the saturated compounds **4a** and **2a** possess remarkable double-bond character. The electron distribution in the 1,3,2-diazaborole **4b** corresponds with that in 6-π-electron systems.

Introduction

The formal substitution of a C=C unit in pyrrole by a B–N group leads to 2,3-dihydro-1*H*-1,3,2-diazaboroles:

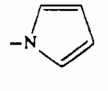

pyrrole

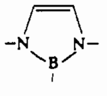

2,3-dihydro-1*H*-1,3,2-diazaborole

The first example of this class of compounds has been synthesized by a catalytic dehydrogenation of a saturated 1,3,2-diazaborolidine by Niedenzu et al. in 1973.[1]

Another simple, universally valid pathway was found by us in 1974, using borolium salts as intermediates:[2,3]

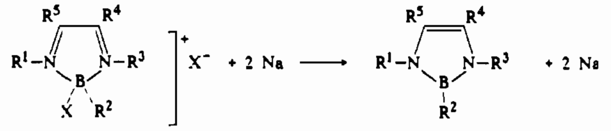

$R^1 = R^3$	R^2	$R^4 = R^5$	X
C_6H_5	CH_3	CH_3	Br
C_6H_5	CH_3	CH_3	Cl
C_6H_5	Br	CH_3	Br
C_6H_5	Cl	CH_3	Cl
$C(CH_3)_3$	CH_3	H	Br
$C(CH_3)_3$	Br	H	Br
$C(CH_3)_3$	Cl	H	Cl

1,3,2-Diazaboroles can act as 6-π-electron ligands in a few chromium complexes:[4,5]

---

[1] Merriam, J. S.; Niedenzu, K. *J. Organomet. Chem.* **1973**, *51*, C1.

0020-1669/90/1329-4421$02.50/0

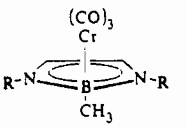

R = $C(CH_3)_3$, $Si(CH_3)_3$

The intent of the investigations, described in this paper, was (1) to synthesize less bulky substituted rings, (2) to study their chemical properties, (3) to carry out a series of X-ray structure determinations, which did not exist for any 1,3,2-diazaborole before, and (4) to evaluate electron density distributions by X–X calculations. A structure determination of 2-chlorine-1,3-dimethyl-1,3,2-diazaborolidine[6] by means of electron diffraction showed the five-membered ring to be planar. The comparison of the X-ray structures of 1,3,2-diazaborolidines with those of unsaturated 1*H*-1,3,2-diazaboroles should give interesting information on similarities and differences in the boron–nitrogen bond.

Experimental Section

Synthesis. All operations were carried out under an atmosphere of pure nitrogen and in dried, freshly distilled solvents using conventional Schlenk techniques.

Synthesis of the 1,3,2-Diazaborolidines. 1,3-Diisopropyl-2-methyl-1,3,2-diazaborolidine (**1a**), 1,3-diethyl-2-methyl-1,3,2-diazaborolidine (**2a**), 1-ethyl-2,3-dimethyl-1,3,2-diazaborolidine (**3a**), and 1,2,3-trimethyl-1,3,2-diazaborolidine (**4a**) are all prepared by method C, using the corresponding ethylenediamines that are lithiated by *n*-butyllithium and then reacted with CH_3BBr_2. As a typical reaction, the synthesis of **1a** is described in detail.

A solution of 28.85 g (200 mmol) of *N*,*N'*-diisopropylethylenediamine in 600 mL of petroleum ether and 150 mL of diethyl ether is cooled to 0 °C. A 160-mL aliquot of a 2.5 M solution of *n*-butyllithium in hexane is added dropwise, and the resulting solution is warmed to room temperature. Further stirring for 10 h at room temperature and boiling for 6 h under reflux complete the reaction. The reaction mixture is cooled to –78 °C, followed by the dropwise addition of 37.13 g (200 mmol) of CH_3BBr_2 in 200 mL of petroleum ether. After warming, about 700 mL of the solvents is distilled off. Thereafter, all volatile components are condensed into a trap (–196 °C) at 80 °C. The condensation products consist of some hexane and **1a**, which is then separated by distillation. Colorless **1a** is collected between 59 and 61 °C (45 Torr). Yield: 23.20 g (69%). Anal. Calcd for $C_9H_{21}BN_2$: C, 64.31; H, 12.59; N, 16.67. Found: C, 63.69; H, 12.41; N, 15.95. ^1H NMR ($CDCl_3$): δ 0.09 (s, 3 H, $-BCH_3$), 1.03 (d, 12 H, $-CH(CH_3)_2$), 3.07 (s, 4 H, $-CH_2CH_2-$), 3.49 (sept, 2 H, $-CH(CH_3)_2$). ^{11}B NMR ($CDCl_3$): δ 32.1. $^{13}C\{^1H\}$ NMR ($CDCl_3$): δ –6.5 ($-BCH_3$), 21.7 ($-CH(CH_3)_2$), 41.6 ($-CH(CH_3)_2$), 44.9 ($-CH_2CH_2-$). Mass: *m*/*z* 168 (M^+).

2a: colorless liquid; bp 89–91 °C (75 Torr); yield 63%. ^1H NMR ($CDCl_3$): δ 0.06 (s, 3 H, $-BCH_3$), 0.99 (t, 6 H, $-CH_2CH_3$), 2.93 (q, 4 H, $-CH_2CH_3$), 3.13 (s, 4 H, $-CH_2CH_2-$). ^{11}B NMR ($CDCl_3$): δ 31.9. $^{13}C\{^1H\}$ NMR ($CDCl_3$): δ –6.0 ($-BCH_3$), 15.0 ($-CH_2CH_3$), 40.7 ($-CH_2CH_3$), 47.4 ($-CH_2CH_2-$). Mass: *m*/*z* 140 (M^+).

3a: colorless liquid; bp 52–54 °C (70 Torr); yield 72%. Anal. Calcd for $C_6H_{15}BN_2$: C, 57.19; H, 12.00; N, 22.23. Found: C, 56.97; H, 11.08; N, 20.56. ^1H NMR ($CDCl_3$): δ 0.05 (s, 3 H, $-BCH_3$), 0.98 (t, 3 H, $-CH_2CH_3$), 2.58 (s, 3 H, $-NCH_3$), 2.92 (q, 2 H, $-CH_2CH_3$), 3.10 (m, 4 H, $-CH_2CH_2-$). ^{11}B NMR ($CDCl_3$): δ 32.5. $^{13}C\{^1H\}$ NMR ($CDCl_3$): δ –8.0 ($-BCH_3$), 14.9 ($-CH_2CH_3$), 33.2 ($-NCH_3$), 40.6 ($-CH_2CH_3$), 47.3 (C(5)), 51.1 (C(4)). Mass: *m*/*z* 126 (M^+).

4a: colorless liquid; bp 75–82 °C (200 Torr); yield 52%. ^{11}B NMR ($CDCl_3$): δ 32.0. Mass: *m*/*z* 112 (M^+). As these data were identical with those of the literature,[1] further identification seemed not to be necessary.

2-Methyl-1-(trimethylsilyl)-1,3,2-diazaborolidine (**5a**), 1-*tert*-butyl-2-methyl-1,3,2-diazaborolidine (**6a**), and 1-isopropyl-2-methyl-1,3,2-diazaborolidine (**7a**) can be prepared by either method A, B, or C. As a typical synthesis by each method, compound **7a** is described.

Method A. A solution of 8.23 g (80.5 mmol) of *N*-isopropylethylenediamine in 100 mL of petroleum ether is added to a solution of 9.18 g (80.5 mmol) of $CH_3B[N(CH_3)_2]_2$ in the same solvent. The reaction mixture is heated to boiling under reflux until no more dimethylamine is evolved. The solvent is distilled off, and the product is separated at 74–76 °C (65 Torr) as a colorless liquid. Yield: 6.35 g (63%). Anal. Calcd for $C_6H_{15}BN_2$: C, 57.19; H, 11.99; N, 22.23. Found: C, 57.45; H, 11.00; N, 22.45. ^1H NMR ($CDCl_3$): δ 0.06 (s, 3 H, $-BCH_3$), 1.02 (d, 6 H, $-CH(CH_3)_2$), 3.13 (m, 4 H, $-CH_2CH_2-$), 3.46 (sept, 1 H, $-CH(CH_3)_2$). ^{11}B NMR ($CDCl_3$): δ 32.7 $^{13}C\{^1H\}$ NMR ($CDCl_3$): δ 21.8 ($-CH(CH_3)_2$), 42.8 (C(4)), 42.9 (C(5)), 44.9 ($-CH(CH_3)_2$). Mass: *m*/*z* 126 (M^+).

5a: colorless liquid; bp 80–83 °C (30 Torr); yield 33%. ^1H NMR ($CDCl_3$): δ 0.10 (s, 9 H, $-Si(CH_3)_3$), 0.13 (s, 3 H, $-BCH_3$), 3.25 (m, 4 H, $-CH_2CH_2-$). ^{11}B NMR ($CDCl_3$): δ 35.9 $^{13}C\{^1H\}$ NMR ($CDCl_3$): δ 0.3 ($-Si(CH_3)_3$), 44.2 (C(4)), 47.5 (C(5)). Mass: *m*/*z* 156 (M^+).

6a: colorless liquid; bp 70–71 °C (22 Torr); yield 67%. Anal. Calcd for $C_7H_{17}BN_2$: C, 60.04; H, 12.23; N, 20.00. Found: C, 59.68; H, 12.70; N, 20.53. ^1H NMR ($CDCl_3$): δ 0.23 (s, 3 H, $-BCH_3$), 1.19 (s, 9 H, $-C(CH_3)_3$), 3.20 (m, 4 H, $-CH_2CH_2-$). ^{11}B NMR ($CDCl_3$): δ 33.5. $^{13}C\{^1H\}$ NMR ($CDCl_3$): δ 30.1 ($-C(CH_3)_3$), 42.4 (C(4)), 46.6 (C(5)), 50.9 ($-C(CH_3)_3$). Mass: *m*/*z* 140 (M^+).

Method B. An 18.57-g (100-mmol) sample of CH_3BBr_2 in 50 mL of pentane is dropped into a mixture of 10.22 g (100 mmol) of *N*-isopropylethylenediamine and 20.24 g (200 mmol) of triethylamine in 200 mL of diethyl ether at –78 °C. After being warmed to room temperature, the reaction mixture is boiled for 1 h under reflux. Solid triethylammonium bromide is filtered out, and the solvent of the solution is distilled off. Boiling point and spectroscopic data agree with those described under method A. Yield: 5.16 g (41%). The syntheses of **5a** and **6a** proceed analogously. Yield: **5a**, 23%; **6a**, 14%.

Method C. An 80-mL aliquot of a 2.5 M solution of *n*-butyllithium in hexane is dropped into a solution of 10.22 g (100 mmol) of *N*-isopropylethylenediamine in 500 mL of petroleum ether and 100 mL of diethyl ether at 0 °C. The reaction mixture is warmed to room temperature to allow evaporation of butane. After the mixture is cooled to –78 °C, 18.57 g (100 mmol) of CH_3BBr_2 in 100 mL of petroleum ether is added dropwise. Warming to room temperature and distilling off 500 mL of the solvents yield a liquid, which is condensed into a trap (–196 °C) at 80 °C. Fractionation gives 4.66 g of **7a** (37%). **5a** and **6a** can be prepared analogously. Yields: **5a**, 11%; **6a**, 17%.

Synthesis of the 2,3-Dihydro-1*H*-1,3,2-diazaboroles. 2,3-Dihydro-1,3,-diisopropyl-2-methyl-1*H*-1,3,2-diazaborole (**1b**), 1,3-diethyl-2,3-dihydro-2-methyl-1*H*-1,3,2-diazaborole (**2b**), and 1-ethyl-2,3-dihydro-1,3-dimethyl-1*H*-1,3,2-diazaborole (**3b**) are prepared by analogous procedures. The synthesis of **1b** is described in detail.

A 12.34-g (73.4-mmol) sample of **1a** is refluxed (210–220 °C) together with 1.9 g of Pd/C catalyst for 6 days. The reaction can be monitored by ^{11}B NMR spectroscopy. The intensity of the **1a** signal at 32 ppm decreases, whereas the signal of **1b** at 27 ppm increases. Distillation at 95–98 °C (50 Torr) yields 10.67 g of **1b** (88%). Anal. Calcd for $C_9H_{19}BN_2$: C, 65.09; H, 11.53; N, 16.87. Found: C, 65.02; H, 11.74; N, 16.85. ^1H NMR ($CDCl_3$): δ 0.43 (s, 3 H, $-BCH_3$), 1.25 (d, 12 H, $-CH(CH_3)_2$), 3.87 (sept, 2 H, $-CH(CH_3)_2$), 6.21 (s, 2 H, $-CH{=}CH-$). ^{11}B NMR ($CDCl_3$): δ 26.7. $^{13}C\{^1H\}$ NMR ($CDCl_3$): δ 24.4 ($-CH(CH_3)_2$), 45.9 ($-CH(CH_3)_2$), 111.5 (C(4), C(5)). Mass: *m*/*z* 166 (M^+).

2b: prepared from 9.85 g of **2a** (9 days of dehydrogenation); colorless liquid; bp 91 °C (75 Torr); yield 65%. Anal. Calcd for $C_7H_{15}BN_2$: C, 60.92; H, 10.95; N, 20.30. Found: C, 59.37; H, 11.39; N, 18.79. ^1H NMR ($CDCl_3$): δ 0.48 (s, 3 H, $-BCH_3$), 1.27 (t, 6 H, $-CH_2CH_3$), 3.51 (q, 4 H, $-CH_2CH_3$), 6.18 (s, 2 H, H(4), H(5)). ^{11}B NMR ($CDCl_3$): δ 26.5. $^{13}C\{^1H\}$ NMR ($CDCl_3$): δ 17.7 ($-CH_2CH_3$), 40.4 ($-CH_2CH_3$), 115.1 (C(4), C(5)). Mass: *m*/*z* 138 (M^+).

3b: prepared from 5.36 g of **3a** (3 days of dehydrogenation); colorless liquid; bp 78–79 °C (72 Torr); yield 86%. Anal. Calcd for $C_6H_{13}BN_2$: C, 58.12; H, 10.57; N, 22.59. Found: C, 58.35; H, 10.90; N, 20.98. ^1H NMR ($CDCl_3$): δ 0.47 (s, 3 H, $-BCH_3$), 1.25 (t, 3 H, $-CH_2CH_3$), 3.21 (s, 3 H, $-NCH_3$), 3.50 (q, 2 H, $-CH_2CH_3$), 6.12 (d, 1 H, H(4)), 6.18 (d, 1 H, H(5)). ^{11}B NMR ($CDCl_3$): δ 26.5. $^{13}C\{^1H\}$ NMR ($CDCl_3$): δ 17.6 ($-CH_2CH_3$), 32.4 ($-NCH_3$), 40.4 ($-CH_2CH_3$), 115 (C(5)), 117 (C(4)). Mass: *m*/*z* 124 (M^+).

2,3-Dihydro-1,2,3-trimethyl-1*H*-1,3,2-diazaborole (**4b**), 2,3-dihydro-2-methyl-1-(trimethylsilyl)-1*H*-1,3,2-diazaborole (**5b**), 1-*tert*-butyl-2,3-dihydro-2-methyl-1*H*-1,3,2-diazaborole (**6b**), and 2,3-dihydro-1-isopropyl-2-methyl-1*H*-1,3,2-diazaborole (**7b**) are synthesized by catalytic dehydrogenation in the gas phase by analogous procedures. Only the synthesis of **7b** is described.

Two 50-mL flasks, each equipped with a stopcock, are connected via a glass tube, which is placed in a tube furnace and filled with 1.5 g of Pd/C catalyst, finely dispersed on glass wool. One of the flasks contains 3.73 g of **7a**. The other is used as a trap and is cooled with liquid nitrogen. The whole apparatus is evacuated, and the tube furnace is heated to 250 °C. The cold flask is connected with a mercury diffusion pump, and pumping is continued during the reaction to pump off hy-

---

(2) Weber, L.; Schmid, G. *Angew. Chem.* **1974**, *86*, 519; *Angew. Chem., Int. Ed. Engl.* **1974**, *13*, 467.

(3) Schmid, G.; Schulze, J. *Chem. Ber.* **1977**, *110*, 2744.

(4) Schmid, G.; Schulze, J. *Angew. Chem.* **1977**, *89*, 258; *Angew. Chem., Int. Ed. Engl.* **1977**, *16*, 249.

(5) Schulze, J.; Schmid, G. *Chem. Ber.* **1981**, *114*, 495.

(6) Seip, H. M.; Seip, R. *J. Mol. Struct.* **1973**, *17*, 361.

drogen. **7b** and unreacted **7a** are condensed into the cold flask. Now the functions of both flasks are changed to repeat the procedure. The reaction is continued until no more **7a** can be registered by ^{11}B NMR spectroscopy, because **7a** and **7b** cannot be separated by distillation. Anal. Calcd for $C_6H_{13}BN_2$: C, 58.12; H, 10.56; N, 22.59. Found: C, 56.32; H, 10.81; N, 22.12. ^{1}H NMR ($CDCl_3$): δ 0.49 (s, 3 H, $-BCH_3$), 1.31 (d, 6 H, $-CH(CH_3)_2$), 3.93 (sept, 1 H, $-CH(CH_3)_2$), 6.27 (m, 2 H, H(4), H(5)). ^{11}B NMR ($CDCl_3$): δ 26.4. $^{13}C\{^1H\}$ NMR ($CDCl_3$): δ 24.4 ($-CH(CH_3)_2$), 46.0 ($-CH(CH_3)_2$), 111.6 (C(5)), 113.2 (C(4)). Mass: *m/z* 124 (M^+).

4b: dehydrogenation temperature 450 °C. Anal. Calcd for $C_5H_{11}BN_2$: C, 55.12; H, 9.25; N, 25.71. Found: C, 53.25; H, 9.29; N, 24.45. ^{1}H NMR (C_6D_6): δ 0.44 (s, 3 H, $-BCH_3$), 2.93 (s, 6 H, $-NCH_3$), 5.99 (s, 2 H, H(4), H(5)). ^{11}B NMR (C_6D_6): δ 26.5. $^{13}C\{^1H\}$ NMR (C_6D_6): δ 32.9 ($-NCH_3$), 117.9 (C(4), C(5)). Mass: *m/z* 110 (M^+).

5b: dehydrogenation temperature 250 °C. Anal. Calcd for $C_6H_{15}BN_2Si$: C, 46.76; H, 9.81; N, 18.17. Found: C, 46.62; H, 10.17; N, 16.32. ^{1}H NMR ($CDCl_3$): δ 0.27 (s, 9 H, $-Si(CH_3)_3$), 0.52 (s, 3 H, $-BCH_3$), 6.22 (pt, 1 H, H(5)), 6.32 (pt, 1 H, H(6)). ^{11}B NMR ($CDCl_3$): δ 30.1. $^{13}C\{^1H\}$ NMR: δ 0.6 ($-Si(CH_3)_3$), 114.9 (C(4)), 116.5 (C(5)). Mass: *m/z* 154 (M^+).

6b: dehydrogenation temperature 250 °C. ^{1}H NMR ($CDCl_3$): δ 0.62 (s, 3 H, $-BCH_3$), 1.44 (s, 9 H, $-C(CH_3)_3$), 6.17 (pt, 1 H, H(5)), 6.35 (pt, 1 H, H(4)). ^{11}B NMR ($CDCl_3$): δ 26.5. $^{13}C\{^1H\}$ NMR: δ 31.6 ($-C(CH_3)_3$), 52.3 ($-C(CH_3)_3$), 110.7 (C(5)), 114.8 (C(4)). Mass: *m/z* 138 (M^+).

Bi(2,3-dihydro-1,2,3-trimethyl-1,3,2-1*H*-diazaborolyl) (8). A 17.2-g (150-mmol) sample of **4a** and 1.9 g of Pd/C catalyst were heated to reflux (210–220 °C) for a period of 4 weeks. After about 12 h, **8** begins to crystallize at the reflux condenser. The dehydrogenation can be observed by ^{11}B NMR spectroscopy, as the signal of **4a** (32.0) decreases, whereas the signal of **8** (26.9) increases. **8** can be isolated by sublimation at 80 °C (10^{-4} Torr) as colorless crystals. Yield: 15.8 g (92%). Anal. Calcd for $C_{10}H_{20}B_2N_4$: C, 55.12; H, 9.25; N, 25.71. Found: C, 55.38; H, 8.77; N, 24.67. ^{1}H NMR (C_6D_6): δ 0.42 (s, 6 H, $-BCH_3$), 2.92 (s, 6 H, N(3)–CH_3, N(3′)–CH_3), 2.96 (s, 6 H, N(1)–CH_3, N(1′)–CH_3), 6.14 (s, 2 H, H(5), H(5′)). ^{11}B NMR (C_6D_6): δ 26.9. $^{13}C\{^1H\}$ NMR (C_6D_6): δ 30.5 (N(3)–CH_3, N(3′)–CH_3), 32.6 (N(1)–CH_3, N(1′)–CH_3), 119.0 (H(5), H(5′)), 121.2 (C(4), C(4′)). Mass: *m/z* 218 (M^+).

Synthesis of the (2,3-Dihydro-η^5-1*H*-1,3,2-diazaborole)tricarbonylchromium Complexes. (2,3-Dihydro-1,3-diisopropyl-2-methyl-η^5-1*H*-1,3,2-diazaborole)tricarbonylchromium (1c). A 1.78-g (6.9-mmol) sample of $(CH_3CN)_3Cr(CO)_3$ and 3.43 g (20.7 mmol) of **1b** are dissolved in 60 mL of dioxane and heated to 60 °C for 4 h. To eliminate free acetonitrile, it was pumped off occasionally. The brown solution is filtered from some solid material, and the dioxane is evaporated under vacuum. The solid residue is stirred with 75 mL of diethyl ether. After filtration the solution is concentrated to 20 mL. Cooling in the refrigerator yields 1.12 g of **1c** (54%) as a yellow powder. Anal. Calcd for $C_{12}H_{19}BCrN_2O_3$: C, 47.71; H, 6.34; N, 9.27; Cr, 17.21. Found: C, 44.47; H, 5.81; N, 9.90; Cr, 17.49. IR (Nujol): 1928 (vs), 1822 (br) cm^{-1}. ^{1}H NMR ($CDCl_3$): δ 0.75 (s, 3 H, $-BCH_3$), 1.26 (d, 12 H, $-CH(CH_3)_2$), 3.42 (sept, 2 H, $-CH(CH_3)_2$), 5.90 (s, 2 H, H(4), H(5)). ^{11}B NMR ($CDCl_3$): δ 17.4. $^{13}C\{^1H\}$ NMR ($CDCl_3$): δ 23.5, 25.0 ($-CH(CH_3)_2$), 51.4 ($-CH(CH_3)_2$), 90.0 (C(4), C(5)), 234.4 (CO). Mass: *m/z* 302 (M^+).

(1,3-Diethyl-2,3-dihydro-2-methyl-η^5-1*H*-1,3,2-diazaborole)tricarbonylchromium (**2c**), (1-ethyl-2,3-dihydro-2,3-dimethyl-η^5-1*H*-1,3,2-diazaborole)tricarbonylchromium (**3c**), (2,3-dihydro-1,2,3-trimethyl-η^5-1*H*-1,3,2-diazaborole)tricarbonylchromium (**4c**), and (4-(2,3-dihydro-1,2,3-trimethyl-1*H*-1,3,2-diazaborol-4-yl)-2,3-dihydro-1,2,3-trimethyl-η^5-1*H*-1,3,2-diazaborolyl)tricarbonylchromium (**9**) are prepared by corresponding methods. Therefore, only the synthesis of **2c** will be described in detail.

A 4.51-g (17.4-mmol) sample of $(CH_3CN)_3Cr(CO)_3$ and 2.82 g (20.4 mmol) of **2b** are stirred in 80 mL of dioxane at room temperature. Volatile material is then evaporated under vacuum. A 40-mL aliquot of dioxane is added, and after the solution is stirred for 15 min at room temperature, it is pumped off under vacuum almost completely. This procedure is repeated with 20, 10, and 5 mL of dioxane. The residue is stirred with 100 mL of diethyl ether, and the mixture is then filtered. The solution is concentrated to about 20 mL to give 1.37 g of amorphous yellow **2c** (29%). Anal. Calcd for $C_{10}H_{15}BCrN_2O_3$: C, 43.83; H, 5.52; N, 10.22; Cr, 18.97. Found: C, 40.65; H, 5.25; N, 10.33; Cr, 19.74. IR (Nujol): 1928 (vs), 1825 (br) cm^{-1}. ^{1}H NMR ($CDCl_3$): δ 0.73 (s, 3 H, $-BCH_3$), 1.19 (t, 6 H, $-CH_2CH_3$), 3.17 (m, 4 H, $-CH_2CH_3$), 5.96 (s, 2 H, H(4), H(5)). ^{11}B NMR ($CDCl_3$): δ 17.3. $^{13}C\{^1H\}$ NMR ($CDCl_3$): δ 17.5 ($-CH_2CH_3$), 45.1 ($-CH_2CH_3$), 92.2 (C(4), C(5)), 234.3 (CO). Mass: *m/z* 274 (M^+).

3c: yellow, amorphous powder; yield 39%. IR (Nujol): 1920 (vs), 1830 (sh), 1821 (vs) cm^{-1}. ^{1}H NMR ($CDCl_3$): δ 0.76 (s, 3 H, $-BCH_3$), 1.21 (t, 3 H, $-CH_2CH_3$), 2.98 (s, 3 H, $-NCH_3$), 3.38 (q, 2 H, $-CH_2CH_3$), 5.93 (s, 2 H, H(4), H(5)). ^{11}B NMR ($CDCl_3$): δ 17.1. Mass: *m/z* 260 (M^+).

4c: yellow, amorphous powder; yield 29%. Anal. Calcd for $C_8H_{11}BCrN_2O_3$: C, 39.06; H, 4.51; N, 11.39; Cr, 21.14. Found: C, 38.89; H, 4.16; N, 12.36; Cr, 21.08. IR (Nujol): 1925 (vs), 1825 (br) cm^{-1}. ^{1}H NMR ($CDCl_3$): δ 0.77 (s, 3 H, $-BCH_3$), 2.97 (s, 6 H, NCH_3), 5.92 (s, 2 H, H(4), H(5)). ^{11}B NMR ($CDCl_3$): δ 17.4. Mass: *m/z* 246 (M^+).

9: yellow powder; yield 80%. Anal. Calcd for $C_{13}H_{20}B_2CrN_4O_3$: C, 44.11; H, 5.70; N, 15.83; Cr, 14.69. Found: C, 43.96; H, 5.77; N, 15.57; Cr, 14.17. IR (Nujol): 1932 (vs), 1851 (vs), 1823 (vs) cm^{-1}. ^{1}H NMR (C_6D_6): δ 0.42 (s, 3 H, $-B'CH_3$), 0.46 (s, 3 H, $-BCH_3$), 2.09 (s, 3 H, N(3)–CH_3), 2.19 (s, 3 H, N(1)–CH_3), 2.57 (s, 3 H, N(3′)–CH_3), 2.77 (s, 3 H, N(1′)–CH_3), 5.09 (s, 1 H, H(5)), 6.91 (s, 1 H, H(5′)). ^{11}B NMR (C_6D_6): δ 16.4 (coordinated ring), 27.5 (uncoordinated ring). Mass: *m/z* 354 (M^+).

(2,3-Dihydro-2-methyl-1-(trimethylsilyl)-1*H*-1,3,2-diazaborolyl)sodium (11a). A solution of 2.56 g (11.3 mmol) of 2,3-dihydro-2-methyl-1,3-bis(trimethylsilyl)-1*H*-1,3,2-diazaborole (**10**)[5] in 10 mL of THF is added dropwise to a −78 °C cold solution of 0.44 g (11.3 mmol) of $NaNH_2$ in 20 mL of THF. As the reaction mixture warms to room temperature, it becomes violet and $(CH_3)_3SiNH_2$ is evolved. All volatile material is pumped off, and the residue is treated with petroleum ether. **11a** (0.35 g) is isolated as a white, pyrophoric powder (19%). ^{1}H NMR (THF-d_8): δ 0.22 (s, 9 H, $-Si(CH_3)_3$), 0.43 (s, 3 H, $-BCH_3$), 6.01 (br, 1 H, H(5)), 6.14 (br, 1 H, H(4)). ^{11}B NMR (THF-d_8): δ 29.8.

(2,3-Dihydro-2-methyl-1-(trimethylsilyl)-1*H*-1,3,2-diazaborolyl)potassium (11b). A solution of 4.10 g (18.1 mmol) of **10**[5] in 50 mL of THF is added dropwise to a solution of 1.83 g (16.3 mmol) of K(O-*t*-Bu) in 50 mL of THF at room temperature. Then the reaction mixture is boiled under reflux for 30 min. The solvent is distilled off almost completely. The residue is dried under vacuum and then treated with petroleum ether. The salt **11b** is isolated as a beige pyrophoric powder. Yield: 2.81 g (81%). Anal. Calcd for $C_6H_{14}BKN_2Si$: C, 37.50; H, 7.34; N, 14.58. Found: C, 35.27; H, 7.03; N, 14.32. ^{1}H NMR (THF-d_8): δ 0.25 (s, 9 H, $-Si(CH_3)_3$), 0.46 (s, 3 H, $-BCH_3$), 6.01 (br, 1 H, H(5)), 6.17 (br, 1 H, H(4)). ^{11}B NMR (THF-d_8): δ 29.8.

Reaction of 11a and 11b with HCl and CH_3OH. **11a** and **11b** react with HCl in diethyl ether or with CH_3OH to give the neutral diazaborole **5b**. Suspensions of **11a** and **11b** in diethyl ether are treated with equimolar amounts of 0.1 M HCl in diethyl ether at −78 °C. After being warmed to room temperature, the solution is filtered from NaCl (KCl) and the solvent is pumped off. **5b** is purified by distillation and characterized by ^{1}H and ^{11}B NMR spectroscopy. The yields vary between 15 and 20%.

The reaction with CH_3OH is carried out in a similar way by addition of an equimolar amount of CH_3OH to an ethereal solution of the salt. **5b** is characterized by comparison of the spectra with that of an authentic probe.

Structural Investigations. Due to the fact that all of the 1,3,2-diazaborolidines and the 2,3-dihydro-1*H*-1,3,2-diazaboroles (besides **8**) are liquids at room temperature, the single crystals necessary for X-ray investigations have been grown on the diffractometer. For that purpose, the compounds have been sealed in glass capillaries (0.2–0.5 mm) under inert gas. The capillaries were adjusted on the goniometer of the diffractometer (Nicolet R3, Mo Kα radiation, graphite monochromator) and cooled below the melting point by means of a cold N_2 gas stream. Under these conditions, a polycrystalline material was formed. Sometimes the liquids solidified as a glass. In these cases an ultrasonic piezocrystal from an old television remote control was attached to the capillary until the glass was transformed into a polycrystalline state. A special apparatus for a miniaturized zone-melting[7] procedure, using focused infrared light as a heat source, enabled the growth of single crystals in the capillary. Table I summarizes the crystallographic data of the investigated compounds.

The symmetry-equivalent reflections have been averaged to independent intensities. A profile fitting has been carried out for the ω-scan data collection of **2a**.[8]

The structure determinations were carried out by the use of direct methods, and the structure refinements, by the block-cascade method of the SHELXTL program or by the full-matrix method of the SHELXTL PLUS program. The atomic form factors of the neutral atoms originate from

---

(7) Brodalla, D.; Mootz, D.; Boese, R.; Osswald, W. *J. Appl. Crystallogr.* **1985**, *18*, 316.

(8) Clegg, W. *Acta Crystallogr.* **1981**, *A37*, 22.

Table I. Crystallographic Data for the Compounds **4a**, **2a**, **4b**, **2b**, and **1b** Together with the Temperatures of Measurement and Crystal Growth (HT = High-Temperature Form; LT = Low-Temperature Form)

compd	V, Å^3	Z	D, g/cm^3	μ, cm^{-1}	M	T, °C	T, °C (cryst growth)	cryst syst	a, Å	b, Å	c, Å	β, deg	2θ, deg	space group
4a	512.13 (54)	3	1.09	0.61	112.01	−161	−37	trigonal	7.373 (3)	7.373 (3)	10.878 (8)	90	3–45, 45–95	$P3_2$
2a (HT)	930.86 (31)	4	1.00	0.55	140.04	−92	−81	monoclinic	16.086 (3)	7.405 (1)	8.911 (2)	118.72 (1)	3–70	Cc
2a (LT)	915.93 (37)		1.02	0.56		−155			16.144 (4)	7.363 (2)	8.796 (2)	118.83 (2)	3–60, 60–90	
4b (HT)	704.21 (27)	4	1.03	0.59	109.97	−73	−37	tetragonal	6.591 (1)	6.591 (1)	16.209 (3)	90	3–40, 40–60	$P4_3$
4b (LT)	683.03 (29)		1.07	0.60		−171			6.518 (1)	6.518 (1)	16.080 (4)	90	3–55, 55–70	
2b	903.13 (86)	4	1.02	0.56	138.02	−103	−73	monoclinic	13.972 (8)	7.448 (4)	8.877 (5)	102.67 (4)	3–40, 40–50	$P2_1/c$
1b	2174.97 (1.02)	8	1.01	0.55	166.08	−150	−50	monoclinic	7.974 (2)	21.498 (6)	12.776 (3)	96.72 (2)	3–70	$P2_1/n$

Table II. Data Refinements

compd	unique intens	no. of obsd intens	no. of refined params	R, %	R_w, %
4a$_1$[a]	3625	1286	124	3.60	3.81
4a$_2$[a]		3301	72	4.23	5.19
4a$_3$[a]		1307	124	3.63	3.91
4a$_4$[b]		3359	72	4.24	5.22
2a HT[c,d]	2376	2339	120	5.25	5.99
2a LT[c,d]	6216	4632	118	5.02	5.46
2a LT$_2$[a,d]		1921	155	3.96	4.60
2a LT$_3$[b,d]		4631	87	4.99	5.31
2a LT$_4$		2548	79	5.79	5.91
2a LT$_5$[b]		2548	51	5.82	5.67
2a LT$_6$		4480	13	5.13	5.39
4b HT[c]	1376	1222	89	5.62	6.30
4b LT[c]	1388	1273	90	4.81	5.48
4b LT$_2$[a]		803	116	3.67	3.97
4b LT$_3$[b]		1273	72	4.74	5.24
2b[c]	1538	1250	119	6.46	6.72
1b[c]	5889	4556	295	5.25	5.42

[a] $2\theta_{max} = 55°$. [b] High-angle refinement. [c] CH_3, CH_2, and CH groups refined as rigid groups. C–H bond length = 0.96 Å; tetrahedral angle at the C atom; temperature parameters of the H atoms are 1.2-fold of the U_{ij} value of the corresponding C atoms or a common temperature parameter for the H atoms of a group. [d] Refinement by damping factor.

Table III. Bond Lengths (Å) and Bond Angles (deg) of **1b**

N(1)–B(2)	1.427 (2)	B(2)–N(3)	1.433 (2)
N(3)–C(4)	1.398 (2)	N(1)–C(5)	1.404 (2)
C(4)–C(5)	1.342 (2)	N(1)–C(6)	1.461 (2)
C(6)–C(7)	1.514 (2)	C(6)–C(8)	1.520 (2)
B(2)–C(9)	1.573 (2)	N(3)–C(10)	1.460 (2)
C(10)–C(11)	1.525 (2)	C(10)–C(12)	1.521 (2)
N(21)–B(22)	1.433 (2)	B(22)–N(23)	1.434 (2)
N(23)–C(24)	1.394 (2)	N(21)–C(25)	1.389 (2)
C(24)–C(25)	1.346 (2)	N(21)–C(26)	1.468 (2)
C(26)–C(17)	1.524 (2)	C(26)–C(28)	1.527 (2)
B(22)–C(29)	1.566 (2)	N(23)–C(30)	1.473 (2)
C(30)–C(31)	1.517 (2)	C(30)–C(32)	1.519 (2)
B(2)–N(1)–C(5)	108.2 (1)	B(2)–N(1)–C(6)	128.8 (1)
C(5)–N(1)–C(6)	123.0 (1)	N(1)–B(2)–N(3)	105.0 (1)
N(1)–B(2)–C(9)	127.6 (1)	N(3)–B(2)–C(9)	127.4 (1)
B(2)–N(3)–C(4)	108.2 (1)	B(2)–N(3)–C(10)	129.2 (1)
C(4)–N(3)–C(10)	122.6 (1)	N(3)–C(4)–C(5)	109.3 (1)
N(1)–C(5)–C(4)	109.3 (1)	N(1)–C(6)–C(7)	112.3 (1)
N(1)–C(6)–C(8)	112.2 (1)	C(7)–C(6)–C(8)	110.0
N(3)–C(10)–C(11)	111.3 (1)	N(3)–C(10)–C(12)	111.5 (1)
C(11)–C(10)–C(12)	110.9	B(22)–N(21)–C(25)	108.5 (1)
B(22)–N(21)–C(26)	129.6 (1)	C(25)–N(21)–C(26)	121.8 (1)
N(21)–B(22)–N(23)	104.7 (1)	N(21)–B(22)–C(29)	127.3 (1)
N(23)–B(22)–C(29)	128.0 (1)	B(22)–N(23)–C(24)	108.1 (1)
B(22)–N(23)–C(30)	129.9 (1)	C(24)–N(23)–C(30)	121.8 (1)
N(23)–C(24)–C(25)	109.5 (1)	N(21)–C(25)–C(24)	109.3 (1)
N(21)–C(26)–C(27)	111.4 (1)	N(21)–C(26)–C(28)	111.5 (1)
C(27)–C(26)–C(28)	111.2	N(23)–C(30)–C(31)	111.3 (1)
N(23)–C(30)–C(32)	111.4 (1)	C(31)–C(30)–C(32)	111.0

ref 9. The reflections were considered as observed with $F_o \geq 3.5\sigma(F)$. The weighting scheme in the least-squares refinement was $w = (\sigma^2(F) + gF^2)^{-1}$. The value of g was determined by fitting $(F_o - F_c)^2$ to $(\sigma^2(F) + gF^2)/k$.

Table IV. Bond Lengths (Å) and Bond Angles (deg) of **2a**

N(1)–B(2)	1.420 (1)	N(1)–C(5)	1.460 (1)
N(1)–C(6)	1.444 (1)	B(2)–C(8)	1.576 (1)
B(2)–N(1′)	1.420 (1)	C(5)–C(5′)	1.534 (2)
C(6)–C(7)	1.522 (1)		
B(2)–N(1)–C(5)	110.4 (1)	B(2)–N(1)–C(6)	129.2 (1)
C(5)–N(1)–C(6)	118.2 (1)	N(1)–B(2)–C(8)	126.1 (1)
N(1)–B(2)–N(1′)	107.9 (1)	C(8)–B(2)–N(1′)	126.1 (1)
N(1)–C(5)–C(5′)	104.5 (1)	N(1)–C(6)–C(7)	113.4 (1)

Table V. Bond Lengths (Å) and Bond Angles (deg) of **2b**

N(1)–B(2)	1.410 (4)	N(1)–C(5)	1.411 (3)
N(1)–C(6)	1.450 (4)	B(2)–N(3)	1.407 (3)
B(2)–C(8)	1.565 (4)	N(3)–C(4)	1.408 (3)
N(3)–C(9)	1.451 (4)	C(4)–C(5)	1.327 (4)
C(6)–C(7)	1.491 (4)	C(9)–C(10)	1.496 (4)
B(2)–N(1)–C(5)	108.2 (2)	B(2)–N(1)–C(6)	131.3 (2)
C(5)–N(1)–C(6)	120.4 (2)	N(1)–B(2)–N(3)	105.9 (2)
N(1)–B(2)–C(8)	127.6 (2)	N(3)–B(2)–C(8)	126.5 (3)
B(2)–N(3)–C(4)	107.9 (2)	B(2)–N(3)–C(9)	130.7 (2)
C(4)–N(3)–C(9)	121.4 (2)	N(3)–C(4)–C(5)	109.5 (2)
N(1)–C(5)–C(4)	108.6 (2)	N(1)–C(6)–C(7)	114.2 (2)
N(3)–C(9)–C(10)	112.9 (2)		

Table VI. Bond Lengths (Å) and Bond Angles (deg) of **4a**

N(1)–B(2)	1.423 (2)	B(2)–N(3)	1.422 (2)
N(3)–C(4)	1.462 (1)	N(1)–C(5)	1.460 (1)
C(4)–C(5)	1.535 (2)	N(1)–C(6)	1.444 (2)
B(2)–C(7)	1.568 (1)	N(3)–C(8)	1.445 (2)
B(2)–N(1)–C(5)	110.1 (1)	B(2)–N(1)–C(6)	128.9 (1)
C(5)–N(1)–C(6)	116.9 (1)	N(1)–B(2)–N(3)	107.8 (1)
N(1)–B(2)–C(7)	126.1 (1)	N(3)–B(2)–C(7)	126.1 (1)
B(2)–N(3)–C(4)	110.0 (1)	B(2)–N(3)–C(8)	129.1 (1)
C(4)–N(3)–C(8)	116.8 (1)	N(3)–C(4)–C(5)	104.1 (1)
N(1)–C(5)–C(4)	104.1 (1)		

Table VII. Bond Lengths (Å) and Bond Angles (deg) of **4b**

N(1)–B(2)	1.446 (2)	B(2)–N(3)	1.450 (2)
N(3)–C(4)	1.407 (2)	N(1)–C(5)	1.409 (2)
C(4)–C(5)	1.362 (3)	N(1)–C(6)	1.468 (2)
B(2)–C(7)	1.578 (2)	N(3)–C(8)	1.464 (2)
B(2)–N(1)–C(5)	108.6 (1)	B(2)–N(1)–C(6)	129.0 (1)
C(5)–N(1)–C(6)	122.4 (1)	N(1)–B(2)–N(3)	104.5 (1)
N(1)–B(2)–C(7)	127.7 (2)	N(3)–B(2)–C(7)	127.8 (2)
B(2)–N(3)–C(4)	108.5 (1)	B(2)–N(3)–C(8)	129.1 (1)
C(4)–N(3)–C(8)	122.3 (1)	N(3)–C(4)–C(5)	109.3 (1)
N(1)–C(5)–C(4)	109.1 (1)		

Preparative Results and Discussion

1,3,2-Diazaborolidines and 1*H*-1,3,2-Diazaboroles. For the preparation of substituted 1*H*-1,3,2-diazaboroles, we selected the method employing the saturated 1,3,2-diazaborolidines, as there are many possibilities for using different nitrogen substituents. The methods to synthesize 1,3,2-diazaborolodines are outlined in

---

(9) *International Tables for X-Ray Crystallography*; Kynoch Press: Birmingham, England, 1969.

Table VIII. Atomic Coordinates ($\times 10^4$) and Equivalent Isotropic Displacement Factors ($Å^2 \times 10^4$) of **1b**

	x	y	z	U_{eq}[a]
N(1)	2213 (1)	1364 (1)	3152 (1)	230 (3)
B(2)	724 (2)	1278 (1)	3655 (1)	228 (3)
N(3)	132 (1)	1894 (1)	3833 (1)	249 (3)
C(4)	1240 (2)	2318 (1)	3448 (1)	281 (4)
C(5)	2466 (2)	2006 (1)	3037 (1)	272 (3)
C(6)	3298 (2)	895 (1)	2751 (1)	249 (3)
C(7)	5156 (2)	1038 (1)	3033 (1)	406 (5)
C(8)	2910 (2)	803 (1)	1567 (1)	397 (5)
C(9)	−99 (2)	645 (1)	3944 (1)	306 (4)
C(10)	−1322 (2)	2090 (1)	4347 (1)	298 (4)
C(11)	−2509 (2)	2501 (1)	3624 (1)	419 (5)
C(12)	−780 (2)	2415 (1)	5389 (1)	452 (5)
N(21)	7165 (1)	930 (1)	9068 (1)	236 (3)
B(22)	7419 (2)	996 (1)	7982 (1)	241 (4)
N(23)	5751 (1)	991 (1)	7424 (1)	267 (3)
C(24)	4601 (2)	926 (1)	8159 (1)	297 (4)
C(25)	5442 (2)	890 (1)	9134 (1)	291 (4)
C(26)	8406 (2)	925 (1)	10012 (1)	267 (3)
C(27)	8157 (2)	365 (1)	10709 (1)	354 (4)
C(28)	8372 (2)	1532 (1)	10630 (1)	440 (5)
C(29)	9142 (2)	1062 (1)	7517 (1)	364 (4)
C(30)	5195 (2)	1084 (1)	6294 (1)	324 (4)
C(31)	3957 (3)	584 (1)	5869 (1)	505 (6)
C(32)	4450 (3)	1728 (1)	6083 (1)	498 (6)

[a] Equivalent isotropic U defined as one-third of the trace of the orthogonalized $\mathbf{U}_{ij}$ tensor.

Table IX. Atomic Coordinates ($\times 10^4$) and Equivalent Isotropic Displacement Factors ($Å^2 \times 10^3$) of **2a**

	x	y	z	U_{eq}[a]
N(1)	715 (1)	314 (1)	2518 (1)	25 (1)
B(2)	0	1449 (1)	2500	23 (1)
C(5)	431 (1)	−1589 (1)	2351 (1)	27 (1)
C(6)	1498 (1)	785 (1)	2232 (1)	32 (1)
C(7)	2455 (1)	212 (1)	3709 (1)	38 (1)
C(8)	0	3590 (1)	2500	34 (1)

[a] Equivalent isotropic U defined as one-third of the trace of the orthogonalized $\mathbf{U}_{ij}$ tensor.

Table X. Atomic Coordinates ($\times 10^4$) and Equivalent Isotropic Displacement Factors ($Å^2 \times 10^4$) of **2b**

	x	y	z	U_{eq}[a]
N(1)	6912 (1)	535 (2)	6569 (2)	551 (7)
B(2)	7777 (2)	470 (3)	5999 (3)	535 (9)
N(3)	7651 (1)	−964 (2)	4942 (2)	488 (6)
C(4)	6728 (2)	−1742 (3)	4910 (3)	517 (7)
C(5)	6287 (2)	−857 (3)	5864 (3)	547 (8)
C(6)	6590 (3)	1785 (4)	7608 (3)	732 (11)
C(7)	6064 (2)	3388 (4)	6829 (3)	749 (11)
C(8)	8694 (2)	1725 (4)	6436 (4)	797 (11)
C(9)	8302 (2)	−1683 (3)	4024 (3)	570 (8)
C(10)	8862 (2)	−3293 (4)	4743 (3)	711 (10)

[a] Equivalent isotropic U defined as one-third of the trace of the orthogonalized $\mathbf{U}_{ij}$ tensor.

Table XI. Atomic Coordinates ($\times 10^4$) and Equivalent Isotropic Displacement Factors ($Å^2 \times 10^4$) of **4a**

	x	y	z	U_{eq}[a]
N(1)	2629 (1)	7581 (1)	−322 (2)	207 (3)
B(2)	635 (2)	7300 (2)	0	195 (4)
N(3)	912 (1)	9293 (1)	318 (2)	205 (3)
C(4)	3067 (2)	10929 (2)	66 (2)	223 (4)
C(5)	4263 (2)	9732 (2)	−69 (2)	219 (4)
C(6)	3277 (2)	6034 (2)	−410 (2)	255 (4)
C(7)	−1493 (2)	5174 (2)	−5 (2)	274 (4)
C(8)	−635 (2)	9944 (2)	407 (2)	257 (4)

[a] Equivalent isotropic U defined as one-third of the trace of the orthogonalized $\mathbf{U}_{ij}$ tensor.

Table XII. Atomic Coordinates ($\times 10^4$) and Equivalent Isotropic Displacement Factors ($Å^2 \times 10^4$) of **4b**

	x	y	z	U_{eq}[a]
N(1)	6354 (2)	3232 (2)	−454	239 (3)
B(2)	6342 (2)	1343 (2)	0 (1)	223 (4)
N(3)	8235 (2)	1355 (2)	456 (1)	243 (3)
C(4)	9284 (2)	3158 (3)	269 (1)	317 (4)
C(5)	8161 (3)	4282 (2)	−268 (1)	314 (5)
C(6)	4783 (3)	4084 (2)	−995 (1)	317 (4)
C(7)	4648 (3)	−348 (3)	0 (2)	365 (5)
C(8)	9088 (3)	−212 (3)	994 (1)	313 (4)

[a] Equivalent isotropic U defined as one-third of the trace of the orthogonalized $\mathbf{U}_{ij}$ tensor.

Table XIII. Synthesized 1,3,2-Diazaborolidines

R^1	R^2	compd	method	yield, %	lit.
$-CH(CH_3)_2$	$-CH(CH_3)_2$	**1a**	C	69	
$-CH_2CH_3$	$-CH_2CH_3$	**2a**	C	63	15
$-CH_2CH_3$	$-CH_3$	**3a**	C	72	
$-CH_3$	$-CH_3$	**4a**	C	52	1, 19
$-Si(CH_3)_3$	H	**5a**	A, B, C	33, 23, 11	
$-C(CH_3)_3$	H	**6a**	A, B, C	67, 14, 17	
$-CH(CH_3)_2$	H	**7a**	A, B, C	63, 41, 37	

Scheme I

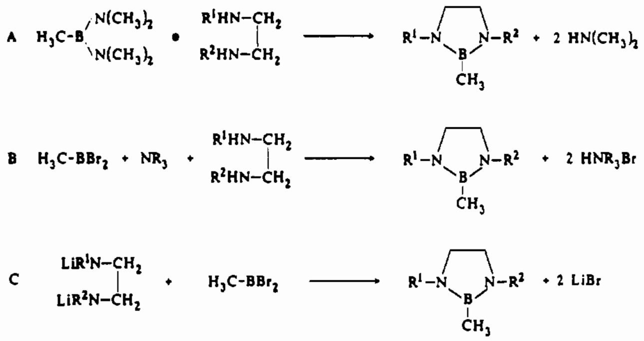

Scheme I.[10-18] Table XIII summarizes the 1,3,2-diazaborolidines, obtained by methods A–C.

The dehydrogenation of compounds **1a**–**3a** succeeds by means of a palladium-active carbon catalyst (Pd/C) under refluxing conditions without solvent. The 1,2,3-trimethyl derivative **4a** as well as the monosubstituted rings **5a**–**7a** are best dehydrogenated in the gas phase by the same catalyst. If **4a** is used in the liquid state, a reaction to form the dimer bi(2,3-dihydro-1,2,3-trimethyl-1,3,2-1*H*-diazaborolyl) (**8**) takes place. The dehydrogenated compounds **1b**–**4b** are all formed in good yields between 65 and 88%, whereas **5b**–**7b** are obtained in minor amounts (37–61%).

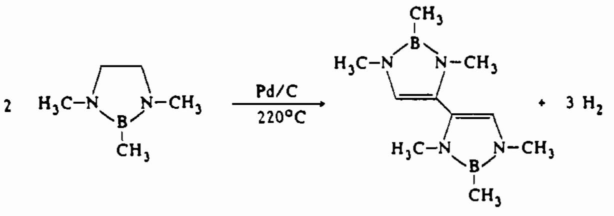

4a **8**

The diazaborolidines as well as the diazaboroles are colorless, air-sensitive liquids, distillable under vacuum conditions. They

---

(10) Nöth, H. *Z. Naturforsch.* **1961**, *16B*, 470.
(11) Niedenzu, K.; Beyer, H.; Dawson, J. W. *Inorg. Chem.* **1962**, *1*, 738.
(12) Fritz, P.; Niedenzu, K.; Dawson, J. W. *Inorg. Chem.* **1964**, *3*, 626.
(13) Niedenzu, K.; Fritz, P.; Dawson, J. W. *Inorg. Chem.* **1964**, *3*, 1077.
(14) Niedenzu, K.; Fritz, P. *Z. Anorg. Allg. Chem.* **1965**, *340*, 329.
(15) Weber, W.; Dawson, J. W.; Niedenzu, K. *Inorg. Chem.* **1966**, *5*, 726.
(16) Brown, M. P.; Dann, A. E.; Hunt, D. W.; Silver, H. B. *J. Chem. Soc.* **1962**, 4648.
(17) Meller, A.; Maracek, H. *Monatsh. Chem.* **1967**, *98*, 2336.
(18) Nöth, H.; Tinhof, W.; Wrackmeyer, B. *Chem. Ber.* **1974**, *107*, 518.
(19) Niedenzu, K.; Miller, C. D. *Fortschr. Chem. Forsch.* **1970**, *15*, 191.

all have been characterized by ^{1}H, ^{11}B, and ^{13}C NMR spectroscopy, by mass spectroscopy, and in most cases by elemental analysis. The data are summarized in the Experimental Section. Only a few comments should be made. Former ^{1}H NMR spectroscopic investigations on 1,3,2-diazaborolidines[20,21] indicate an almost planar molecular structure of the five-membered heterocycles and herewith support the interpretation of vibrational spectra of these and similar compounds.[22-26] The 1,3,2-diazaborolidines all show the resonance signals for the ring protons in the range 3.0–3.2 ppm. The range for the CH_2 protons in the disubstituted examples **5a–7a** varies between 3.1 and 3.3 ppm. Due to the unequivalency of the N atoms, the CH_2 signals form unresolved multiplets.

The ^{13}C NMR spectra show a significant influence of the N substituents on the chemical shift of the ring carbon atoms. Unsymmetrically substituted rings therefore show two different signals for C(4) and C(5). The ^{11}B NMR signals of 1,3,2-diazaborolidines indicate no visible dependency on the substituents. They are observed between about 32 and 33 ppm. Only for the derivative **5a** is a low-field shift observed, due to the electronic withdrawing effect of the $Si(CH_3)_3$ group. The transition from the saturated diazaborolidines to the unsaturated 1*H*-diazaboroles causes a low-field shift for the ring protons of about 3 ppm, which is now in the range 6–6.3 ppm. As can be expected, the unsymmetrically substituted rings show two different signals for the protons in the 4- and 5-positions.

The signals for the carbon atoms C(4) and C(5) are found in the expected region for sp^2-hybridized carbon atoms in perturbed aromatic systems (>100 ppm) and agree with values found for other 1*H*-1,3,2-diazaboroles. Compared with the case of diazaborolidines, there is a low-field shift of about 48 ppm. Pyrrolidines and pyrrole behave in the same manner.[27] The dependency of the ^{13}C NMR shifts of C(4) and C(5) on the substituent is to be compared with that found for the saturated rings. The increasing inductive effect of the substituents is accompanied by an increase of the shielding (e.g. 111.5 ppm for $N-C(CH_3)_3$, 117.5 ppm for $N-CH_3$).

The ^{11}B NMR spectra show that the B atoms in 1*H*-1,3,2-diazaboroles are better shielded than those in 1,3,2-diazaborolidines. The signals are found between 26 and 27 ppm, except for those of the $Si(CH_3)_3$ derivative **5b**. The electron-withdrawing silyl group causes a low-field shift to 30.1 ppm.

Complexation Reactions. As shown, 1*H*-1,3,2-diazaboroles can act as 6-π-electron ligands:[4,5]

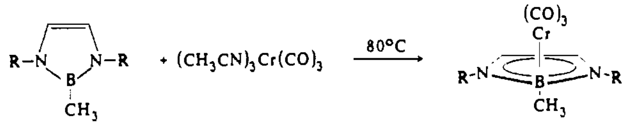

Under comparable conditions, a complex with the trimethyl-substituted ring **4b** cannot be isolated. This suggests that the ligands are responsible for the stability of the complexes. To test this hypothesis, we tried to use the 1*H*-1,3,2-diazaboroles **1b–7b** for complexation reactions under varied conditions in dioxane. The results are summarized in Table XIV.

As can be seen, the bulkiest substituted ring, **1b**, gives the best yields at 60 °C. **2b–4b** must be reacted at room temperature with $(CH_3CN)_3Cr(CO)_3$ to give yields of only 29 and 39%, respectively. The monosubstituted rings **5b–7b** mainly lead to unidentified decomposition products, but in no case to the expected $Cr(CO)_3$ complexes. The dimer molecule **8** acts as a good ligand, using only one ring for metal coordination.

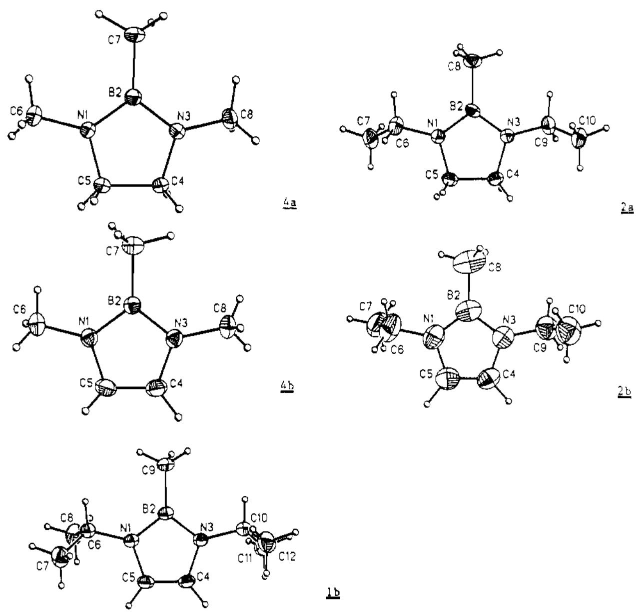

Figure 1. Molecular structures of the 1,3,2-diazaborolidines **4a** and **2a** and the 2,3-dihydro-1*H*-1,3,2-diazaboroles **4b**, **2b**, and **1b**.

Table XIV. Formation Conditions of 1*H*-1,3,2-Diazaborole–Tricarbonylchromium Complexes

		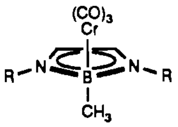	
1*H*-1,3,2-diazaborole	*T*, °C	no.	yield, %
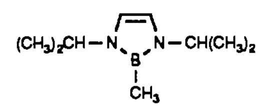 **1b**	60	**1c**	54
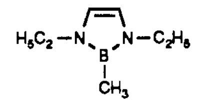 **2b**	20	**2c**	29
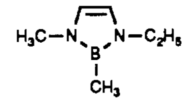 **3b**	20	**3c**	39
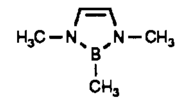 **4b**	20	**4c**	29
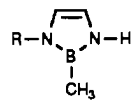 **5b–7b** R = $Si(CH_3)_3$, $C(CH_3)_3$, $CH(CH_3)_2$	20		

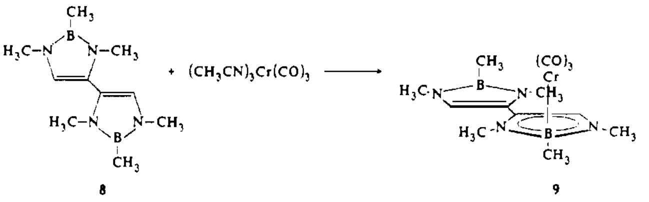

8 **9**

N-silylated 1,3,2-diazaboroles possess an interesting preparative potential, as the $Si(CH_3)_3$ groups can be substituted by alkali

---

(20) Niedenzu, K.; Miller, C. D.; Smith, S. L. *Z. Anorg. Allg. Chem.* **1970**, *372*, 337.
(21) Abel, E. W.; Bush, R. P. *J. Organomet. Chem.* **1965**, *3*, 245.
(22) Goubeau, J.; Zappel, A. *Z. Anorg. Allg. Chem.* **1955**, *279*, 38.
(23) Goubeau, J.; Schneider, H. *Liebigs Ann. Chem.* **1964**, *675*, 1.
(24) Dawson, J. W.; Fritz, P.; Niedenzu, K. *J. Organomet. Chem.* **1966**, *5*, 211.
(25) Niedenzu, K.; Dawson, J. W.; Fritz, P. *Z. Anorg. Allg. Chem.* **1966**, *342*, 297.
(26) Niedenzu, K.; Fritz, P. *Z. Anorg. Allg. Chem.* **1966**, *344*, 329.
(27) Abraham, R. J.; Loftus, P. *Proton and Carbon-13 NMR-Spectroscopy*; Heyden-Verlag: London, 1978.

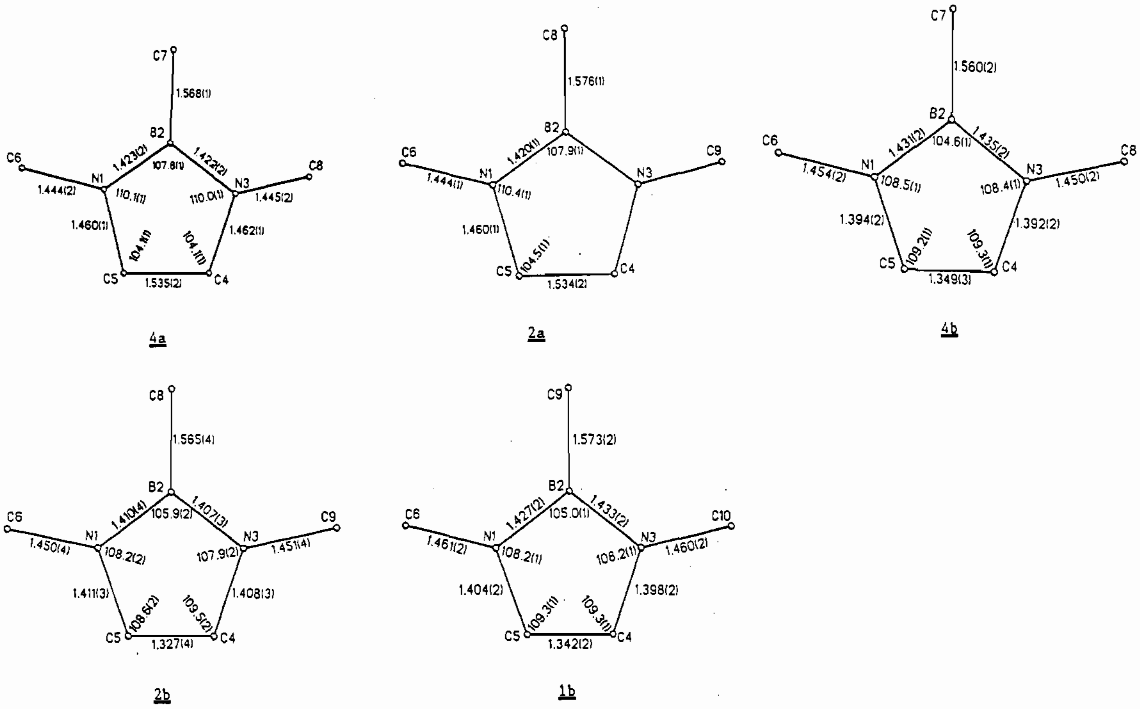

Figure 2. Simplified molecular structures of **4a**, **2a**, **4b**, **2b**, and **1b** with important bond lengths (Å) and bond angles (deg).

metals. By use of the former described 1,3,2-diazaborole, compound **10**, one silyl group can be substituted either by means of $NaNH_2$ or by K(O-*t*-Bu). The sodium and potassium compounds

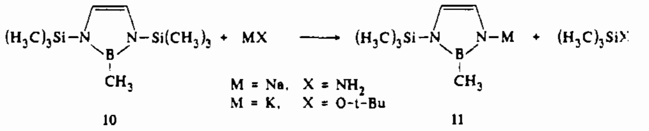

11a and **11b** can be isolated as pyrophoric, colorless powders. These salt-like systems promise to be powerful complexation educts.

Proton-active compounds like HCl or CH_3OH can be used to generate the monosubstituted azaborole ring **5b**. The yields are

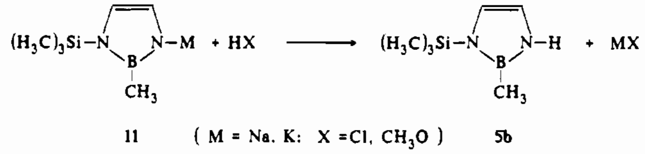

low (18–23%), as decomposition reactions accompany the protonation. Preliminary experiments using the 1,3,2-diazaborole anion as a ligand in transition-metal complexes are promising. The existence of a few pyrrolyl complexes with manganese and iron, where the pyrrolyl ring acts as a η^5 ligand,[28-31] should be noted.

The yellow complexes **1c**–**4c** darken at room temperature in the course of some days, indicating a beginning decomposition. Their ^1H NMR spectra are characterized by a high-field shift of the ring protons of about 0.2 ppm, compared to those of the free rings. This high-field shift is smaller than could be expected from the experience with an arene–tricarbonylchromium compound.[32] The shifts in analogous pyrrole complexes amount to ca. 0.5 ppm, compared to those of the free pyrrole.[33] The small effect in **1c**–**4c** can be explained by the strong σ-donor and the weaker π-acceptor capacities in comparison with those of arenes. Electron-pushing substituents in arene complexes also cause a less strong high-field shift. The only ring proton in the coordinated ring in **9** shows a remarkable high-field shift of about 1 ppm. This loss of shielding may be due to a conjugation between both rings.

^{13}C NMR spectra could only be registered for complexes **1c** and **2c**, as the methyl derivatives are too unstable for longer measurements. The ring carbon atoms of **1c** and **2c** show a high-field shift in the expected range, indicating that they participate in the interaction with the chromium atom. The low-field shift of the CO signals, compared with that of $Cr(CO)_6$, can be observed in all (η^6-arene)$Cr(CO)_3$ complexes.[34,35] The effect increases with increasing donor capacities of the ligands. From these data one can conclude that the 1*H*-1,3,2-diazaboroles are strong electron donors.

The combination of a BN moiety with a transition metal in most cases leads to a considerable high-field shift of the ^{11}B NMR signals. This is also valid for complexes **1c**–**4c**. The ^{11}B NMR signals are observed between 17.1 and 17.4 ppm, showing a difference as compared to the signals of the free rings of about 9 ppm. Thus, complex **9** shows two signals at 16.4 ppm for the coordinated ring and at 27.5 ppm for the free ring. Similar results have been found for the formerly described complexes.[4,5] The metalation of the 1*H*-1,3,2-diazaboroles by Na and K causes only a very small high-field shift in comparison with the case of the NH compound **5b**.

X-ray Structures

Figure 1 shows the molecular structures of the investigated 1,3,2-diazaborolidines and 2,3-dihydro-1*H*-1,3,2-diazaboroles. In Figure 2 important bond lengths and bond angles are shown in simplified structures.

Bond distances and bond angles in the saturated compounds **4a** and **2a** are almost the same within standard deviations. Going from the saturated 1,3,2-diazaborolidines to the corresponding unsaturated 1,3,2-diazaboroles, of course, the C(4)–C(5) bond lengths shorten considerably due to the change of a single to a double bond. The C(4)–C(5) double bond in **4b**, **2b**, and **1b** varies only insignificantly between about 1.33 and 1.35 Å. The change

---

(28) Joshi, K. K.; Pauson, P. L.; Qazi, A. R.; Stubbs, W. H. *J. Organomet. Chem.* **1964**, *1*, 471.

(29) Joshi, K. K.; Pauson, K. L. *Proc. Chem. Soc., London* **1962**, 326.

(30) Pauson, P. L.; Qazi, A. R. *J. Organomet. Chem.* **1967**, *7*, 321.

(31) Kuhn, N.; Horn, E.-M.; Boese, R.; Augart, N. *Angew. Chem.* **1988**, *100*, 1433; *Angew. Chem., Int. Ed. Engl.* **1988**, *27*, 1368.

(32) Magini, A.; Taddei, F. *Inorg. Chim. Acta* **1968**, *2*, 8.

(33) Öfele, K.; Dotzauer, E. *J. Organomet. Chem.* **1971**, *30*, 211.

(34) Bodner, G. M.; Todd, L. J. *Inorg. Chem.* **1974**, *13*, 360.

(35) Bodner, G. M.; Todd, L. J. *Inorg. Chem.* **1974**, *13*, 1335.

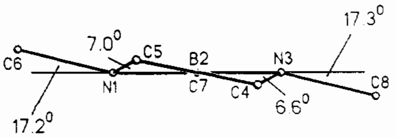

Figure 3. Deviations from the NBN plane in **4a**.

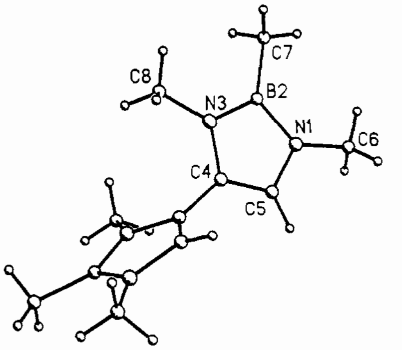

Figure 4. Molecular structure of **8**.

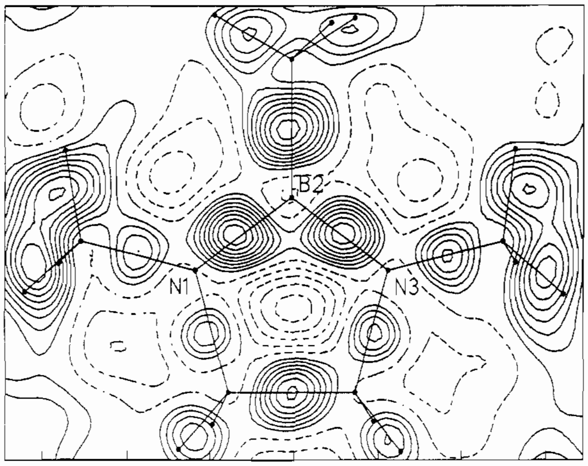

Figure 5. Difference electron density in the NBN plane of **4a**. Contour lines are in e/Å^3; min = −0.55; max = 0.37. Distance: positive 0.05 e/Å^3, negative 0.1 e/Å^3 (dotted). Reference line: first solid line.

from the 1,3,2-diazaborolidines to the 1,3,2-diazaboroles does not cause any remarkable influence on the B–N bond length. It is found between 1.41 and 1.43 Å, as in most aminoboranes. Consequently, the B–N distances are not suited to recognize influences of the substituents.

The boron atoms in the 1,3,2-diazaborolidines **4a** and **2a** are sp^2-hybridized, as can be seen from the sum of the bonding angles at the boron atoms, which is 360° in both cases. However, the sum of the bonding angles at the N atoms is only 355.9° (**4a**) and 357.8° (**2a**), indicating a distorted-trigonal-planar geometry. We interpret this effect by the existence of the sp^3-hybridized ring C atoms, which are positioned outside the NBN plane. The methyl groups in **4a** are bent in the same direction by 17.8°; the ring C atoms, by 6.6 and 7.0°, respectively. The situation in **4a** is shown in Figure 3. The conditions in the ethyl derivative **2a** are quite similar.

In contrast to these results, the 1*H*-1,3,2-diazaboroles consist of planar rings. The boron as well as the nitrogen atoms in **4b**, **2b**, and **1b** show sp^2 hybridization, as can be shown by the sum of the angles at these atoms.

The molecular structure of the dimer **8** will also be discussed briefly. It is shown in Figure 4. The two five-membered rings are linked via a σ bond between the C(4) atoms. The ring planes form an interplanar angle of 70°. A free rotation along the C(4)–C(4′) bond is not possible, as the methyl substituents at the N(3) atoms are too bulky. The B–N bonds in **8** are observed between 1.425 and 1.428 Å. The methyl groups at the N(3) positions of the two rings are found 8.1° outside the ring planes, due to their steric interaction.

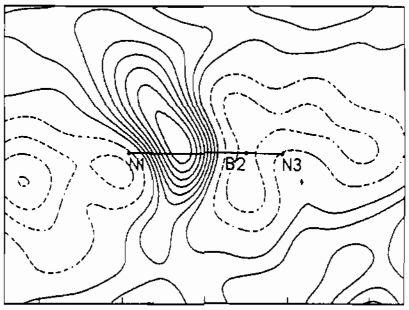

Figure 6. Difference electron density along the N1–B2 bond through the maximum. Contour lines are in e/Å^3; min = 0.54, max = 0.41. Distance: positive 0.05 e/Å^3, negative 0.1 e/Å^3 (dotted). Reference line: first solid line.

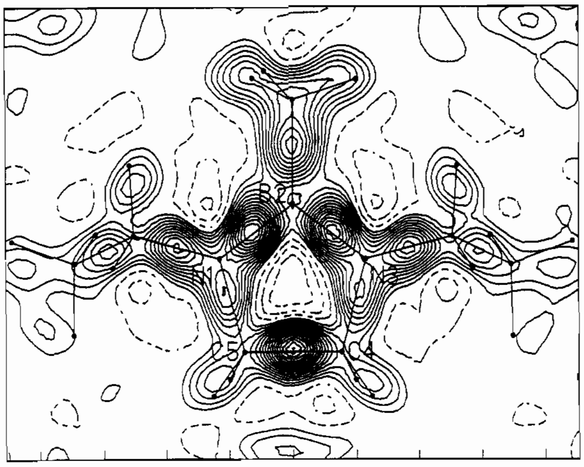

Figure 7. Difference electron densities in the NBN plane of **2a**. Contour lines are in e/Å^3; min = −0.37, max = 0.78. Distance: positive 0.05 e/Å^3, negative 0.1 e/Å^3 (dotted). Reference line: first solid line.

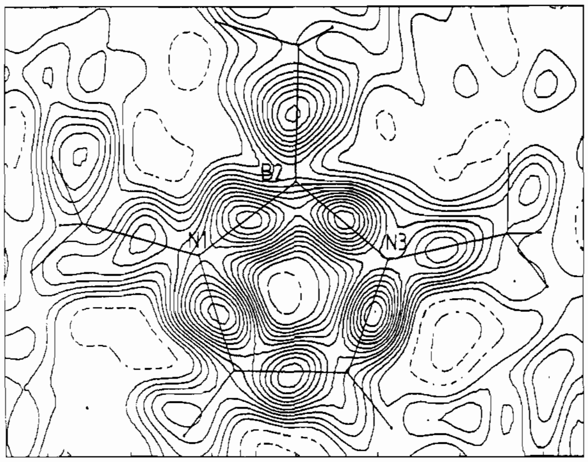

Figure 8. Difference electron density in the NBN plane of **4b**. Contour lines are in e/Å^3; min = −0.13, max = 0.33. Distance: positive 0.025 e/Å^3, negative 0.05 e/Å^3 (dotted). Reference line: first solid line.

Electron Densities

The difference electron densities of 1,2,3-trimethyl-1,3,2-diazaborolidine (**4a**), 1,3-diethyl-2-methyl-1,3,2-diazaborolidine (**2a**), and 2,3-dihydro-1,2,3-trimethyl-1*H*-1,3,2-diazaborole (**4b**) show that the B–N bonds in the saturated compounds **4a** and **2a** possess a remarkable double-bond character and, moreover, that the electron distribution in the diazaborole **4b** corresponds with that in 6-π-electron systems. The maxima of the bonding electron densities are found to be not exactly on the connecting line of the atomic nuclei. In **4a** and **2a** these maxima are shifted to the nitrogen atoms, due to the different electronegativities of N and B. The most interesting electron density of 1,2,3-trimethyl-1,3,2-diazaborolidine (**4a**) is shown in Figure 5. It has been calculated for the plane constructed by the nitrogen and boron

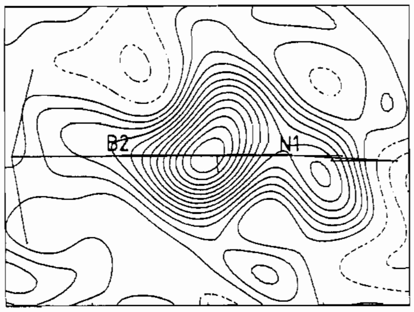

Figure 9. Difference electron density perpendicular to the NBN plane in **4b** through the N1–B2 bond. Contour lines are in e/Å^3; min = –0.17, max = 0.32. Distance: positive 0.025 e/Å^3, negative 0.05 e/Å^3 (dotted). Reference line: first solid line.

atoms. The bonding electrons of the B–C, B–N, and the C–C bonds are situated in the calculated plane. The highest calculated density is 0.37 e/Å.[3] The maxima are found a little outside of the ring, as could be expected for sp^2-hybridized N atoms. But, there are some doubts if this finding is really significant.

Figure 6 shows the deformation electron density perpendicular to the N–B–N plane along one of the B–N bonds in **4a**. The elliptic inclination of the electron density perpendicular to the B–N bond is caused by the B–N π-back-bonding.

As can be seen from Figure 7, the maxima of the bonding electrons in the NBN plane of 1,3-diethyl-2-methyl-1,3,2-diazaborolidine (**2a**) are found exactly on the connecting line of the N(1)–B(2), B(2)–N(3), C(4)–C(5), and B(2)–C(8) nuclei. Again, the maxima in the B–N bonds are shifted toward the N atoms, due to their higher electronegativity.

The electronic difference between the saturated 1,3,2-diazaborolidines **4a** and the "aromatic" system of 1*H*-1,3,2-diazaboroles is elucidated in Figure 8. The difference electron density in the NBN plane of **4b** is similar in all five bonds. The shift of the maxima in the B–N bonds toward the nitrogen atoms cannot be observed to the same extent as in the diazaborolidines, due to the extensive delocalization of the π electrons.

Supplementary Material Available: Listings of thermal parameters, atomic coordinates, detailed crystallographic descriptions, and all bond lengths and angles (26 pages); tables of calculated and observed structure factors (110 pages). Ordering information is given on any current masthead page.

Contribution No. 5279 from the Central Research and Development Department,
Experimental Station, E. I. du Pont de Nemours & Company, Inc., Wilmington, Delaware 19880-0328

Steric Effects in Polypyrazolylborates: Mixed Complexes M(HB(3-isopropyl-4-bromopyrazolyl)$_3$)L

Joseph C. Calabrese, Peter J. Domaille, Jeffery S. Thompson,* and Swiatoslaw Trofimenko

Received December 7, 1989

The stable, tetrahedral M(HB(3-isopropyl-4-bromopyrazolyl)$_3$)Cl, (= ML*Cl) complexes react with uninegative polydentate ligands L, forming mixed species ML*L, the structure of which depends on the nature of L. With L = [HB(pyrazolyl)$_3$]$^-$ or [HB(3,5-Me$_2$pyrazolyl)$_3$]$^-$, octahedral complexes are obtained, as was established by the paramagnetic NMR spectra of the Co(II) derivatives and an X-ray crystallographic structure determination of NiL*(HB(pyrazolyl)$_3$). This complex, $C_{39}H_{47}B_2Br_3N_{12}Ni$, crystallizes in the monoclinic space group $P2_1/m$ with two molecules per unit cell of dimensions a = 9.764 (2) Å, b = 16.804 (4) Å, c = 13.673 (5) Å, and β = 96.35 (2)°, at –70 °C. Least-squares refinement of 280 variables led to a value of the conventional R index (on F) of 0.044 and of R_w of 0.042 for 2546 reflections with $I > 3.0\sigma(I)$. The Ni(II) ion is coordinated to six pyrazolyl nitrogen atoms from two different ligands. The reaction with [HB(3-Phpyrazolyl)$_3$]$^-$ produced ML*L complexes where L was coordinated via two 3-phenylpyrazolyl groups and an agostic B–H–M bond, as was established by X-ray crystallography for the Co(II) compound. This complex, $C_{51}H_{53}B_2Br_3CoN_{12}$, crystallizes in the orthorhombic space group *Pbca* with eight molecules per unit cell of dimensions a = 22.269 (3) Å, b = 22.299 (3) Å, and c = 21.216 (5) Å, at –70 °C. Least-squares refinement of 607 variables led to a value of the conventional R index (on F) of 0.062 and of R_w of 0.047 for 2722 reflections with $I > 3.0\sigma(I)$. The Co(II) ion is coordinated to five pyrazolyl nitrogen atoms from two ligands and a hydrogen atom from the [HB(3-Phpyrazolyl)$_3$]$^-$ group. Bidentate dipyrazolylborates [H$_2$B(pyrazolyl)$_2$]$^-$ and [H$_2$B(3,5-Me$_2$pyrazolyl)$_2$]$^-$ produced ML*L complexes where L coordinated through two pyrazolyl groups, and through an agostic B–H–M bond, as was established by X-ray crystallography for CoL*(H$_2$B(3-Phpyrazolyl)$_2$). This complex, $C_{48}H_{53}B_2Br_3CoN_{10}$, crystallizes in the triclinic space group $P\bar{1}$ with two molecules per unit cell of dimensions a = 11.343 (1) Å, b = 11.426 (1) Å, c = 20.716 (6) Å, α = 80.74 (1)°, β = 80.80 (1)°, and γ = 74.25 (1)°, at –70 °C. Least-squares refinement of 577 variables led to a value of the conventional R index (on F) of 0.064 and of R_w of 0.068 for 5695 reflections with $I > 3.0\sigma(I)$. The Co(II) ion is coordinated to five pyrazolyl groups from two ligands and a hydrogen atom from the [H$_2$B(3-Phpyrazolyl)$_2$]$^-$ ligand. The complex CoL*(Ph$_2$B(pyrazolyl)$_2$) was shown to lack an agostic interaction. This complex, $C_{48}H_{53}B_2Br_3CoN_{10}$, crystallizes in the monoclinic space group $P2_1/m$ with two molecules in a unit cell of dimensions a = 10.570 (1) Å, b = 16.717 (4) Å, c = 14.918 (4) Å, and β = 108.35 (1)°, at –70 °C. Least-squares refinement of 316 variables led to a value of the conventional R index (on F) of 0.055 and of R_w of 0.045 for 2064 reflections with $I > 3.0\sigma(I)$. The Co(II) ion is coordinated to five pyrazolyl groups from two ligands. With L = [B(3-Phpyrazolyl)$_4$]$^-$, the ML*L complex with M = Ni(II) had a five-coordinate structure, while that for M = Co(II) was tetrahedral. Simple bidentate ions such as acetylacetonate, tropolonate, and diethyldithiocarbamate produced five-coordinate ML*L species, whereas the oxalate ion gave the binuclear, bis(five-coordinate), M$_2$(L*)$_2$(C$_2$O$_4$) complex.

Introduction

The ability to synthesize, in controlled fashion, transition-metal complexes containing several different ligands is an important desideratum in coordination chemistry. From that point of view, a gap existed in the area of polypyrazolylborate ligands, where among the plethora of reported complexes[1] only a few ML*L compounds are represented, containing one [RB(pz*)$_3$]$^-$ (=L*) and a different polydentate ligand, L. No examples have been reported for first-row transition metals,[2] and examples for second row metals as, for instance, Ru(B(pz)$_4$)(η^6-C$_6$H$_6$)$^+$ and Rh(HB(pz)$_3$)(η^5-C$_5$H$_5$)$^+$ contain only carbocyclic π-donors as L.[3] They

---

(1) (a) Trofimenko, S. *Prog. Inorg. Chem.* **1986**, *34*, 115–210. (b) Trofimenko, S. *Chem. Rev.* **1972**, *72*, 497–509. (c) Trofimenko, S. *Acc. Chem. Res.* **1971**, *4*, 17–22.

(2) Two compounds, Cu(HB(3,5-Me$_2$pz)$_3$)(R$_2$NCS$_2$) (Thompson, J. S.; Marks, T. J.; Ibers, J. A. *J. Am. Chem. Soc.* **1979**, *101*, 4180–4192) and Co(p-BrC$_6$H$_4$B(pz)$_3$)(HB(3,5Me$_2$pz)$_3$) (cited in ref 1a as a personal communication) have been mentioned, but not structural proof or experimental data were given.

0020-1669/90/1329-4429$02.50/0 © 1990 American Chemical Society